Am J Physiol Regul Integr Comp Physiol 314: R122–R134, 2018.
First published September 20, 2017; doi:10.1152/ajpregu.00176.2017.

RESEARCH ARTICLE | *Respiration*

A mitohormetic response to pro-oxidant exposure in the house mouse

Yufeng Zhang,[1] Frances Humes,[1] Gregory Almond,[2] Andreas N. Kavazis,[3] and Wendy R. Hood[1]

[1]*Department of Biological Science, Auburn University, Auburn, Alabama;* [2]*Department of Clinical Sciences, College of Veterinary Medicine, Auburn University, Auburn, Alabama; and* [3]*School of Kinesiology, Auburn University, Auburn, Alabama*

Submitted 8 May 2017; accepted in final form 11 September 2017

Zhang Y, Humes F, Almond G, Kavazis AN, Hood WR. A mitohormetic response to pro-oxidant exposure in the house mouse. *Am J Physiol Regul Integr Comp Physiol* 314: R122–R134, 2018. First published September 20, 2017; doi:10.1152/ajpregu.00176.2017.—Mitochondria are hypothesized to display a biphasic response to reactive oxygen species (ROS) exposure. In this study, we evaluated the time course changes in mitochondrial performance and oxidative stress in house mice following X-irradiation. Forty-eight mice were equally divided among six groups, including a nonirradiated control and five experimental groups that varied in time between X-ray exposure and euthanasia (1 h and 1, 4, 7, and 10 days after X-irradiation). We measured parameters associated with mitochondrial respiratory function and ROS emission from isolated liver and skeletal muscle mitochondria and levels of oxidative damage and antioxidants in liver, skeletal muscle, and heart tissues. Mitochondrial function dropped initially after X-irradiation but recovered quickly and was elevated 10 days after the exposure. Hydrogen peroxide production, lipid peroxidation, and protein carbonylation showed inverse U-shaped curves, with levels returning to control or lower than control, 10 days after X-irradiation. Enzymatic antioxidants and markers for mitochondrial biogenesis exhibited a tissue-specific response after irradiation. These data provide the first chronological description of the mitohormetic response after a mild dose of irradiation and highlight the protective response that cells display to ROS exposure. This study also provides valuable information and application for future mitochondrial and oxidative stress studies in numerous physiological settings.

mitohormesis; mitochondrial function; oxidative stress

INTRODUCTION

In eukaryotic cells, mitochondria are important intracellular organelles that support both the energetic demands of the body and exert regulatory control over many physiological processes. Reactive oxygen species (ROS) have been proposed to be an inevitable by-product of oxidative phosphorylation (OXPHOS), with OXPHOS contributing the majority of ROS (i.e., superoxide) production that occurs within cells (2). Much of the ROS that are produced are quickly quenched by antioxidants (46, 55). When ROS production exceeds the capacity of cells to reduce their reactivity, cells are said to experience oxidative stress (51). When cells experience oxidative stress, lipids, proteins, and DNA become damaged, and this damage may ultimately reduce cellular performance and contribute to senescence (11). As a result, there has been growing interest in oxidative stress in diverse fields of biology and physiology (11, 38).

Despite its popularity, the notion that oxidative stress is always harmful is controversial (1, 16, 36, 53). The major criticisms include the point that ROS act as signaling molecules that mediate cellular and systemic physiological changes (50). For example, many transcriptional factors or proteins, such as nuclear factor E2-related factor 2 (NFE2l2), microtubule-associated proteins 1A/1B light chain 3B (LC3B), nuclear respiratory factor (Nrf1), and peroxisome proliferator-activated receptor gamma coactivator 1-α (PGC-1α), are regulated by ROS. These pathways regulate, among others, antioxidant defense systems, cell cycle, survival and metabolism, and inflammation (40, 57). In addition, damage from ROS does not consistently have a negative impact on cell function and bioenergetic capacity. A number of studies indicated that oxidative damage to protein, lipid, or DNA can be repaired, and damaged molecules can be recycled (7, 9, 12). As a result, modest levels of oxidative stress can be associated with damage that is ephemeral (62), whereas signaling processes can improve mitochondria and cellular function (15). Since high levels of uncontrolled ROS remain harmful (47), one must conclude that elevated ROS can have a positive or negative impact on physiological processes. Just as exposure to some toxins can have beneficial effects at low levels, whereas high levels could be damaging (i.e., hormesis) (4, 34), the same principle appears to apply to ROS exposure (47). Mitohormesis is the biphasic reaction that is predicted to occur in response to free-radical accumulation in the cell (47, 61). Low levels of free-radical production are expected to stimulate resistance to ROS damage and increase longevity (47). Conversely, high levels of free-radical production are expected to contribute to the accumulation of damage that ultimately reduces longevity. Whereas the mitohormetic response has been supported by several studies, the mechanisms responsible for mitohormesis are poorly understood.

To study mitohormesis, it is important to choose an appropriate pro-oxidant for experimental studies. A variety of techniques have been used to increase ROS production in experimental studies. Yet, many methods, particularly that rely on the use of toxic chemicals, such as paraquat or diquat, have negative impacts on cells that extend beyond simply increasing in ROS and localize in select tissues, resulting in broad-spectrum tissue damage and a significant risk of death for experimental subjects (25). In contrast, radiation induces a systemic increase in ROS in animals by the direct ionization of water found in cells and organs throughout the body (55). Radiation induces oxidative stress both directly (e.g., ionization of water) and indirectly (e.g., causing mitochondria damage, leading to increased mitochondrial ROS emission). Specifically, X-irradiation has been shown to stimulate oxidative

Address for correspondence and present address: Y. Zhang, Buck Institute for Research on Aging, 8001 Redwood Blvd., Novato, CA 94945 (e-mail: yzhang@buckinstitute.org).

stress in cell culture (28, 48), laboratory rodents (45), and wild animals (13). The use of radiation as a pro-oxidant generator has many advantages (3). Irradiation can generate a system-wide increased ROS when the whole organism is exposed uniformly or a tissue- or organ-specific increase when exposure is focused and targeted (44). In addition, the level of ROS generated can be controlled by adjustment of the dosage (27).

METHODS

Basic care and ethical approval. Adult (4–6 mo old), female, wild-derived house mice (*Mus musculus*) were used in this experiment. These mice are descended from individuals that were obtained from Dr. Wayne Potts at the University of Utah and were 19 generations removed from the wild. Wild-derived animals have many advantages compared with laboratory counterparts; most importantly, wild-derived animals are more responsive and sensitive to stressors compared with laboratory animals (14, 17). The experiment was conducted in May 2016, when animals were maintained on a natural light-dark cycle (~17–7) and temperature (average 30/17°C). Standard rodent chow (Teklad Global Diet 2019; Envigo, Somerset, NJ) and water were provided ad libitum throughout the experimental period, and all animals were provided with a running wheel as enrichment. All husbandry and experimental procedures were approved by the Auburn University Institutional Animal Care and Use Committee (PRN 2016-2903).

Experimental design, X-irradiation, and dissection. Mice were randomly assigned to one of six groups (n = 8/group) under the condition that mice in each group were from different parental lineages to ensure genetic diversity. Group was defined by time euthanized relative to the X-irradiation. All mice, excluding the controls, were X-irradiated in a rodent plastic transport cage (37.3 × 23.4 × 14.0 cm; Innovive, San Diego, CA) using the PRIMUS linear accelerator (Siemens, Munich, Germany) at the Radiology Laboratory in the Auburn University College of Veterinary Medicine. During irradiation, a thin layer of plastic was taped in place, just above the backs of the mice, to ensure an even dosage of radiation throughout whole animal's body. Irradiation schedules were staggered to ensure that all mice were age matched throughout groups. All X-irradiated mice were irradiated at a dose rate of 2 Gy/min for 2½ min to achieve a total dosage of 5 Gy. Dosage of X-irradiation was chosen by information from literature and preliminary studies in the laboratory. Commonly used laboratory mouse strains display levels of tolerance to radiation—50% lethal dose of an exposed population within 30 days range from 6.5 to 9 Gy (58). Preliminary studies using 1, 2, and 5 Gy of X-irradiation indicated that the dosage of 5 Gy resulted in better mitochondrial function, 7 days postirradiation, and thus, 5 Gy was deemed most appropriate for this investigation. After irradiation, mice were euthanized 1 h and 1, 4, 7, and 10 days later.

At each time point, mice were anesthetized with an overdose of isoflurane vapors and then swiftly decapitated with a rodent guillotine. The left lateral and right medial lobe of the liver and the skeletal muscle of the right hindlimb (including major muscle groups tibialis anterior, soleus, gastrocnemius, quadriceps, and hamstrings; hereafter, "muscle") were dissected for immediate mitochondria isolation. At the same time, the rest of the liver, left hindlimb muscle, and heart were quickly removed, placed into a microcentrifuge tube, and flash frozen in liquid nitrogen before being moved to a −80°C freezer for future analyses.

Mitochondria isolation. Mitochondria were isolated following a protocol detailed in Hyatt et al. (19) and Mowry et al. (39). Briefly, the combined left lateral and right medial lobe of the liver was weighed and put into a liver isolation solution (250 mM sucrose, 5 mM HEPES, 1 mM EGTA) at a ratio of 1:10 and minced with scissors. This minced tissue was further homogenized with a Potter-Elvehjem PTFE pestle and glass tube. The resulting homogenate was centrifuged for 10 min at 500 *g* at 4°C, pelleting the cellular debris. The supernatant was then decanted through a cheesecloth filter and centrifuged for 10 min at 3,500 *g* at 4°C, pelleting the mitochondrial fraction. The supernatant was removed and the pellet resuspended in the liver isolation solution. This solution was centrifuged for 10 min at 3,500 *g* at 4°C, the supernatant discarded, and the final mitochondrial pellet suspended in mannitol-sucrose solution (220 mM mannitol, 70 mM sucrose, 10 mM Tris·HCl, and 1 mM EGTA, pH 7.4).

Muscle was also weighed and put in a muscle isolation solution (100 mM KCl, 40 mM Tris·HCl, 10 mM Tris base, 1 mM $MgSO_4$, 0.1 mM EDTA, 0.2 mM ATP, and 2% free fatty acid BSA, pH 7.40) at a ratio of 1:10. Muscles were minced with scissors and then homogenized for 5 s with a VIRTUS polytron at 12,000 rpm. Trypsin (5 mg/g wet muscle) was added and mixed continually for 7 min to digest the minced muscle. This reaction was terminated with the addition of another 1:10 ratio of muscle-to-muscle isolation solution. The homogenate was centrifuged at 500 *g* for 10 min at 4°C, pelleting down cellular debris. The supernatant was decanted through cheesecloth and centrifuged at 3,500 *g* for 10 min to pellet the mitochondrial fraction. The supernatant was discarded and the remaining mitochondrial pellet resuspended in muscle isolation solution. This was then centrifuged at 3,500 *g* for 10 min. The supernatant was discarded, and the pellet was resuspended in non-BSA solution (same as muscle isolation solution but without BSA) at a ratio of 1:10. This resuspended pellet was centrifuged at 3,500 *g* for 10 min. Finally, the mitochondrial pellet was suspended in a mannitol-sucrose solution.

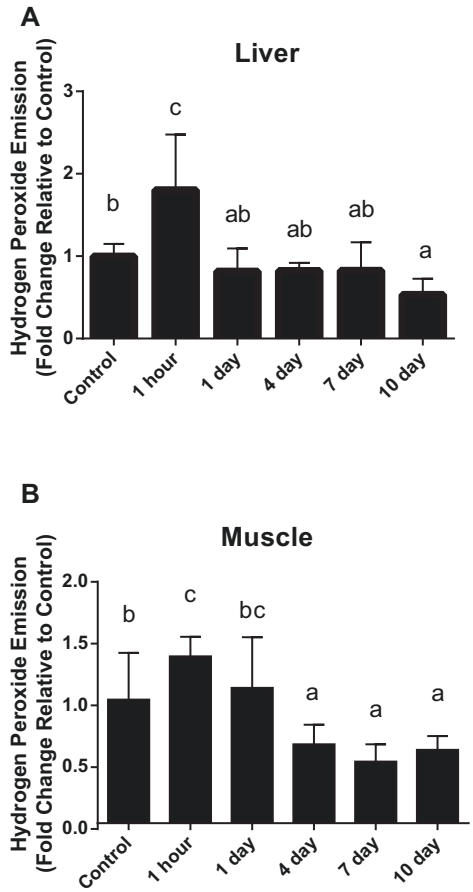

Fig. 1. Hydrogen peroxide emission by isolated mitochondria collected from (*A*) liver and (*B*) muscle of mice. Tissues were collected from nonirradiated control mice and from mice, 1 h and 1, 4, 7, and 10 days postirradiation. SD bars are given (n = 8/group). Bars with different superscripts are significantly different.

Mitochondrial respiration. Isolated mitochondria (20 μl) were incubated in 1 ml respiration buffer (100 mM KCl, 50 mM MOPS, 10 mM KH_2PO_4, 20 mM glucose, 10 mM $MgCl_2$, 1 mM EGTA, and 0.2% free fatty acid BSA, pH 7.0) at 37°C, and respiration rates were determined polarographically (Oxytherm; Hansatech Instruments, Norfolk, UK). In chamber 1, mitochondrial respiration was measured using 2 mM pyruvate, 2 mM malate, and 2 mM glutamate (hereafter, complex I substrate). In chamber 2, mitochondrial respiration was measured using 5 mM succinate with 5 μM rotenone to inhibit complex I (hereafter, complex II substrate). The state 3 respiration was initiated by the addition of 0.25 mM ADP to the respiration chamber containing mitochondria and respiratory substrates. State 4 respiration was recorded following the phosphorylation of ADP. States 3 and 4 respiration rates were normalized to mitochondrial citrate synthase (CS) activity. The respiratory control ratio (RCR) was calculated by dividing state 3 by state 4. The presence of mitochondrial hexokinases during our state 4 measurements could have allowed for some cycling of ATP–ADP, resulting in a slightly elevated state 4 and thus slightly lower RCR values.

ROS emission. ROS emission, in isolated mitochondria, was determined using Amplex Red (catalog number A22188; Thermo Fisher Scientific, Waltham, MA). Details of this assay have been described previously (21, 29). Briefly, this assay is based on the concept that horseradish peroxidase catalyzes the hydrogen peroxide-dependent

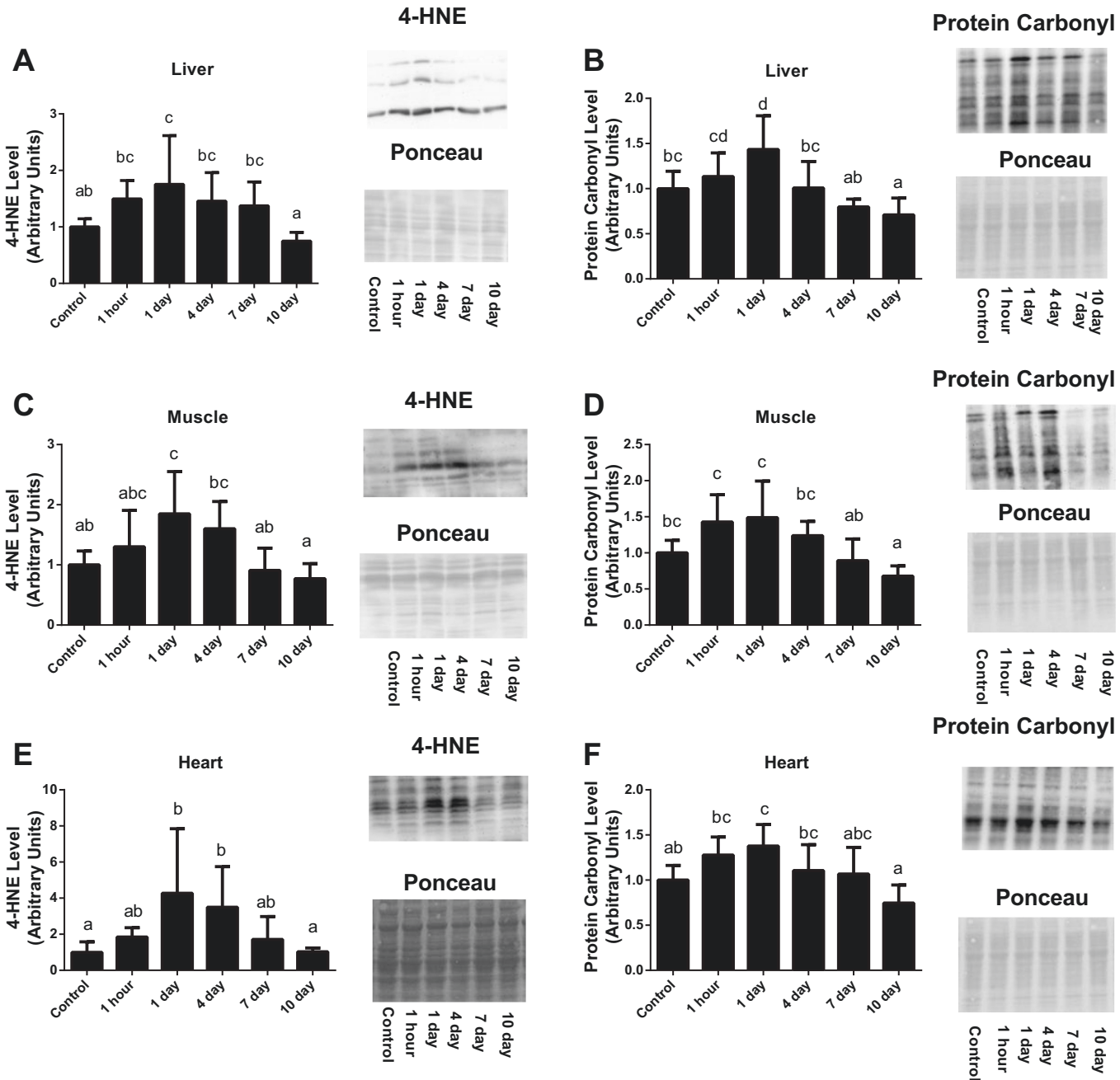

Fig. 2. Relative levels of 4-hydroxynonenal (4-HNE)-conjugated proteins, indicating lipid peroxidation, and protein carbonyls, indicating oxidative damage to proteins, in liver (*A* and *B*, respectively), muscle (*C* and *D*, respectively), and heart (*E* and *F*, respectively) of mice. Tissues were collected from nonirradiated control mice and from mice, 1 h and 1, 4, 7, and 10 days postirradiation. SD bars are given (n = 8/group). Bars with different superscripts are significantly different. Representative Western blot images are shown to the right of the graphs.

Table 1. *Respiration rate from isolated mitochondria in liver and muscle collected from mice*

	State 3				State 4			
	Liver		Muscle		Liver		Muscle	
	Complex I substrate	Complex II substrate	Complex I substrate	Complex II substrate	Complex I substrate	Complex II substrate	Complex I substrate	Complex II substrate
Control	133.17 ± 59.47	214.62 ± 70.38	83.22 ± 13.38	113.35 ± 72.81	17.49 ± 6.87	33.08 ± 17.34	19.25 ± 4.34	60.21 ± 43.77
1 h	84.22 ± 40.90	166.13 ± 43.18	92.98 ± 29.10	157.16 ± 90.49	13.99 ± 2.69	29.36 ± 5.90	24.82 ± 7.86	87.18 ± 56.64
1 Day	111.04 ± 42.96	160.64 ± 74.31	140.65 ± 31.05	248.06 ± 99.74	13.91 ± 5.82	31.03 ± 14.44	28.19 ± 9.54	129.58 ± 44.32
4 Days	108.23 ± 33.67	174.33 ± 66.43	124.20 ± 81.56	114.46 ± 59.25	16.32 ± 6.15	28.89 ± 13.99	32.58 ± 20.97	50.27 ± 25.99
7 Days	110.72 ± 44.88	204.94 ± 73.27	97.55 ± 54.13	101.45 ± 40.02	14.94 ± 4.56	29.71 ± 8.27	24.86 ± 17.16	55.15 ± 33.61
10 Days	119.74 ± 28.97	206.58 ± 27.08	135.22 ± 92.53	153.95 ± 57.39	13.77 ± 2.24	29.13 ± 8.70	29.02 ± 24.70	61.30 ± 32.02

Means ± SD are given (n = 8/group). Respiration rate (pmol O_2 · min^{-1} · citrate synthase $unit^{-1}$). Tissues include those collected from nonirradiated control mice and from mice, 1 h and 1, 4, 7, and 10 days postirradiation. No significant differences were observed.

oxidation of nonfluorescent Amplex Red to fluorescent resorufin red. Approximately 1 μg/μl mitochondria was added in the assay buffer containing 100 mM KCl, 5 mM KH_2PO_4, 1 mM EGTA, 10 mM $MgCl_2$, 50 mM MOPS, and 0.2% free fatty acid BSA in the presence of exogenous SOD (40 U/ml), horseradish peroxidase (10 U/ml), and Amplex Red (0.05 mM). We monitored resorufin formation at an excitation wavelength of 545 nm and an emission wavelength of 590 nm using the Synergy H1 Hybrid plate reader (BioTek; Winooski, VT). We recorded readings of resorufin formation every 5 min for 30 min, and a slope (i.e., rate of formation) was produced. The slope obtained was converted into the rate of hydrogen peroxide production with a standard curve and normalized to mitochondrial CS activity.

Western blot. We used Western blot to quantify the relative expression of the proteins listed below in the liver, muscle, and heart samples. We followed the protocol of the Western blot described in Mowry et al. (39). Briefly, these measures included the protein-bound 4-hydroxynonenal (4-HNE), a marker of lipid peroxidation (ab46545; Abcam, Cambridge, MA), and protein carbonyls, a marker of protein damage (OxyBlot s7150; EMD Millipore, Billerica, MA). Furthermore, the relative protein levels of the enzymatic antioxidants copper-zinc SOD (CuZnSOD; GTX100554; GeneTex, Irvine, CA), manganese SOD (MnSOD; GTX116093; GeneTex), glutathione peroxidase 1 (GPX-1; GTX116040; GeneTex), and catalase (GTX110704; GeneTex) were determined**.** In addition, the relative protein levels of Nrf1 (GTX103179; GeneTex), NFE2l2 (GTX103322; GeneTex), PGC-1α (GTX37356; GeneTex), and microtubule-associated proteins 1A/1B LC3B (GTX127375; GeneTex) were determined. Each Western membrane was stained by ponceau, and protein content of these blots was normalized to ponceau stain levels (the loading and transfer control). A chemiluminescent system was used to visualize marked proteins (GE Healthcare Life Sciences, Pittsburgh, PA). Images were taken and analyzed with the ChemiDoc-It Imaging System (UVP, Upland, CA).

Mitochondrial complex activity. The activity of electron transport system complexes was quantified using an enzymatic assay, as described by Kavazis et al. (21). Mitochondria, isolated from liver and

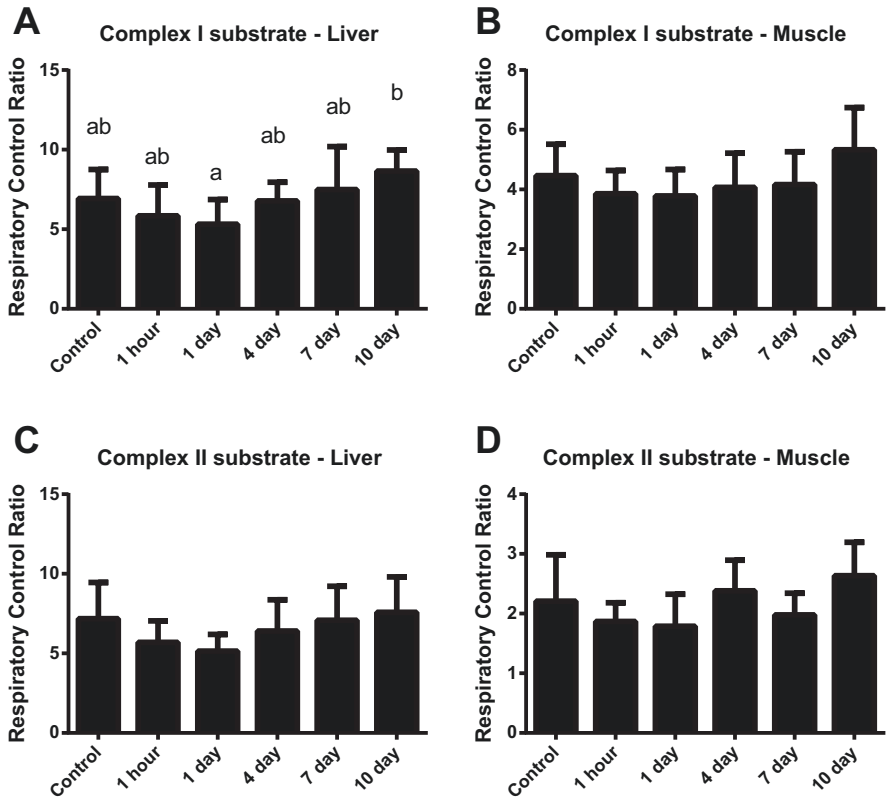

Fig. 3. Respiratory control ratio for mitochondria isolated from liver using glutamate, pyruvate, and malate (complex I) (*A*) or succinate (complex II) (*C*) as substrate and from muscle using glutamate, pyruvate, and malate (complex I) (*B*) or succinate (complex II) (*D*) of mice. Tissues were collected from nonirradiated control mice and from mice, 1 h and 1, 4, 7, and 10 days postirradiation. SD bars are given (n = 8/group). Bars with different superscripts are significantly different.

muscle, were subjected to three cycles of freezing and thawing to lyse membranes before analysis. Complex I (NADH dehydrogenase) enzyme activity was measured as a function of the decrease in absorbance from NADH oxidation by decylubiquinone, before and after the addition of rotenone. Complex II (succinate dehydrogenase) activity was measured as a function of the decrease in absorbance from 2,6-dichloroindophenol reduction. Complex III (ubiquinol cytochrome *c* oxidoreductase) activity was determined as a function of the increase in absorbance from cytochrome c reduction. Complex IV (cytochrome *c* oxidoreductase) activity was determined as a function of the decrease in absorbance from cytochrome c oxidation. Specificity of complex IV activity was determined by the monitoring of changes in absorbance in the presence of potassium cyanide. CS was measured in isolated mitochondria as a function of the increase in absorbance from 5,5′-dithiobis-2-nitrobenzoic acid reduction. Enzyme activities were normalized to mitochondrial CS activity.

Tissues were homogenized, and protein content was determined by the method of Bradford. Then, the CS activity of the liver, muscle, and

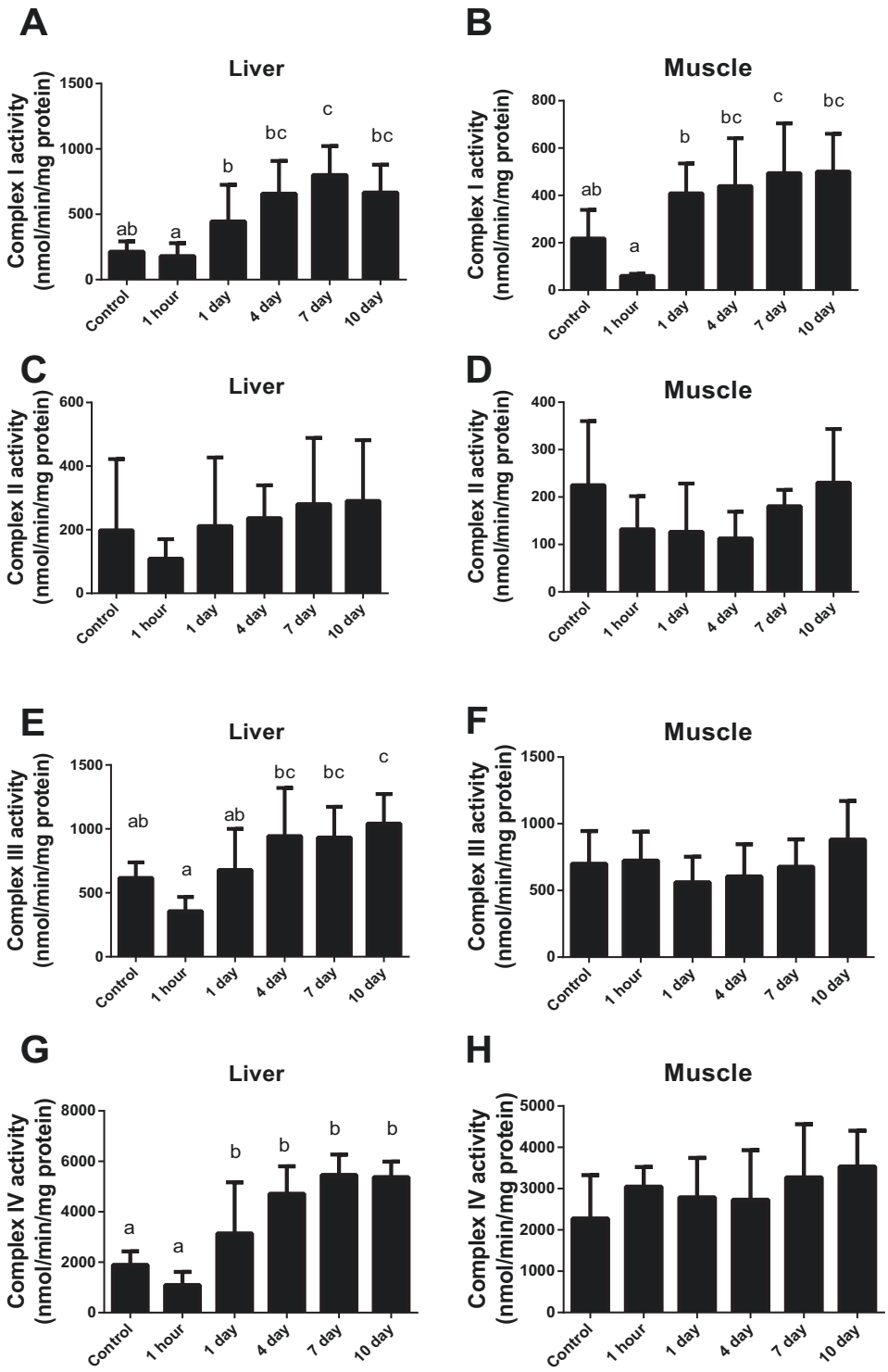

Fig. 4. Activity of the mitochondrial electron transport system enzyme complexes isolated from the liver and muscle of mice. Activity measurements include complexes I (*A*), II (*C*), III (*E*), and IV (*G*) in liver and complexes I (*B*), II (*D*), III (*F*), and IV (*H*) in muscle. Tissues were collected from nonirradiated control mice and from mice, 1 h and 1, 4, 7, and 10 days postirradiation. SD bars are given (n = 8/group, except control n = 7). Bars with different superscripts are significantly different.

heart was measured in tissue homogenates, and it was normalized to tissue protein content.

Statistical analyses. All statistical tests were completed using SigmaStat 3.5 (Systat Software, San Jose, CA). ANOVA was used to compare treatment groups. When appropriate, a Tukey honest significant difference post hoc test was performed to identify differences among groups. Significance was established at $P < 0.05$.

RESULTS

ROS emission. We measured H_2O_2 levels as a proxy for ROS emission by the mitochondria. Our data showed that X-irradiation resulted in significant changes in isolated liver and muscle mitochondrial ROS emission. In both tissues, relative H_2O_2 emission levels were higher than the control, 1 h after irradiation. Liver mitochondrial ROS emission returned to control values at *day 1* but dropped even lower at *day 10* ($F_{5,47} = 11.9$, $P < 0.001$; Fig. 1*A*). Muscle mitochondrial ROS emission returned to control levels at *day 1* but then dropped below control values at *day 4* and remained at these new levels until *day 10* ($F_{5,47} = 16.2$, $P < 0.001$; Fig. 1*B*).

Oxidative damage. The protein levels for markers for lipid oxidative damage (4-HNE) and protein oxidative damage (protein carbonyl) were measured in liver, muscle, and heart. All showed similar trends but varied in the day of maximum expression. Liver, muscle, and heart 4-HNE levels were higher than control on *day 1* (liver: $F_{5,47} = 9.02$, $P < 0.001$, Fig. 2*A*; muscle: $F_{5,47} = 5.02$, $P = 0.001$, Fig. 2*C*; heart: $F_{5,47} = 6.12$, $P < 0.001$, Fig. 2*E*). 4-HNE levels started to dropped and reached controls levels by *day 4* (liver and muscle) or *day 7* (heart).

Liver, muscle, and heart protein levels were higher than control on *day 1* in liver and heart, and by *day 10*, these levels were lower than control (liver: $F_{5,47} = 6.12$, $P < 0.001$, Fig. 2*B*; heart: $F_{5,47} = 8.89$, $P < 0.001$, Fig. 2*F*). In muscle, protein carbonyl levels increased above control values (albeit not significant) and dropped below control values by *day 10* (muscle: $F_{5,47} = 10.7$, $P < 0.001$; Fig. 2*D*).

Mitochondrial respiratory function and complex activity. The RCR is a representative measure of the functional and coupled state of mitochondria and represents the ability of the electron transport system to respond to available ADP. States 3 and 4, using both complexes I and II substrates, did not vary among groups (Table 1). Liver RCR displayed a U-shape relationship with complex I substrate, with the lowest point occurring 1 day after irradiation and highest point occurring 10 days after irradiation ($F_{5,47} = 3.23$, $P = 0.014$; Fig. 3*A*). The pattern for muscle RCR with complex II substrate was not significant ($F_{5,47} = 1.838$, $P = 0.126$; Fig. 3*C*). In muscle, RCR with complexes I and II substrates displayed similar patterns, but neither was significant (complex 1 substrate: $F_{5,47} = 2.15$, $P = 0.080$, Fig. 3*B*; complex II substrate: $F_{5,47} = 2.26$, $P = 0.066$, Fig. 3*D*).

The enzymatic activities of complexes I, II, III, and IV were measured in isolated mitochondria. In liver, complexes I, III, and IV all displayed an increase in activity following irradiation. Specifically, complex I activity increased above control at *day 7* ($F_{5,46} = 9.54$, $P < 0.001$; Fig. 4*A*), complex III activity increased above control at *day 10* ($F_{5,47} = 8.59$, $P < 0.001$; Fig. 4*E*), and complex IV activity increased above control at *day 1* ($F_{5,47} = 23.3$, $P < 0.001$; Fig. 4*G*). In muscle, the pattern for complex I mirrored that of the liver ($F_{5,47} = 11.0$, $P < 0.001$; Fig. 4*B*), but no other significant changes were observed (Fig. 4, *D*, *F*, and *H*).

Tissues can also compensate for a decline in mitochondria function by an increase of the number of mitochondria present through mitochondrial biogenesis. In our study, mitochondrial content, as estimated by CS activity, did not differ over time in the liver, muscle, or heart (Table 2).

Changes in the relative protein expression. NFE2l2 levels in the liver and heart were significantly higher for *days 4–10* postirradiation, relative to the control, 1 h, and 1 day postirradiation (liver: $F_{5,47} = 9.67$, $P < 0.001$, Fig. 5*A*; heart: $F_{5,47} = 7.44$, $P < 0.001$, Fig. 5*E*). Muscle displayed a similar relationship with a more gradual increase in expression from 1 h to 4 days ($F_{5,47} = 9.67$, $P < 0.001$; Fig. 5*C*). LC3B levels in the liver and muscle were significantly higher at *day 1* postirradiation compared with *day 10* (liver: $F_{5,47} = 2.854$, $P = 0.025$, Fig. 5*B*; muscle: $F_{5,47} = 7.499$, $P < 0.001$, Fig. 5*D*). In the heart, LC3B levels were the highest at 1 h postirradiation and dropped back to the control level at *day 4* ($F_{5,47} = 6.363$, $P < 0.001$; Fig. 5*F*). In the muscle, Nrf1 levels were higher at *days 7* and *10* compared with 1 h postirradiation ($F_{5,47} = 6.389$, $P < 0.001$; Fig. 6*C*). In the heart, *day 10* mice had higher Nrf1 levels compared with control, 1 h, and 1 day postirradiation. Furthermore, *day 7* mice had higher Nrf1 levels than *day 1* mice ($F_{5,47} = 8.735$, $P < 0.001$; Fig. 6*E*). In muscle, *day 1* postirradiation had significantly lower PGC-1α levels than *day 10* ($F_{5,47} = 3.7$, $P = 0.007$; Fig. 6*D*). In the heart, PGC-1α levels dropped after irradiation but returned to control levels at *day 4* ($F_{5,47} = 10.55$, $P < 0.001$; Fig. 6*F*).

A significant decrease in the relative expression of GPX was observed at 1 h postirradiation, and that was maintained through *day 10* in both liver and muscle (liver: $F_{5,47} = 11.5$, $P < 0.001$, Fig. 7*A*; muscle: $F_{5,47} = 11.6$, $P < 0.001$, Fig. 7*C*). Catalase levels in liver showed a similar pattern to GPX (liver: $F_{5,47} = 5.65$, $P < 0.001$; Fig. 7*B*), and catalase levels in muscle were the highest at *day 1* but then decreased and were similar to control levels by *day 7* ($F_{5,47} = 6.91$, $P < 0.001$; Fig. 7*D*). GPX (Fig. 7*E*) and catalase (Fig. 7*F*) in the heart stayed relatively constant throughout the time course study.

Table 2. *Mitochondrial content in 3 tissues collected from mice tissues*

	Control	1 h	1 Day	4 Days	7 Days	10 Days	*P*
Liver	833 ± 220	771 ± 148	797 ± 162	933 ± 366	840 ± 281	1,003 ± 184	0.51
Muscle	1,318 ± 403	1,523 ± 405	1,330 ± 409	1,634 ± 442	1,482 ± 397	1,399 ± 258	0.33
Heart	2,368 ± 694	1,863 ± 599	2,215 ± 519	1,960 ± 440	2,395 ± 803	1,918 ± 523	0.29

Means ± SD are given ($n = 8$/group). Tissues include those collected from nonirradiated control mice and from mice, 1 h and 1, 4, 7, and 10 days postirradiation. Mitochondrial content was based on citrate synthase activity (nmol · min^{-1} · mg protein^{-1}). No significant differences were observed. *P* values for each ANOVA are given.

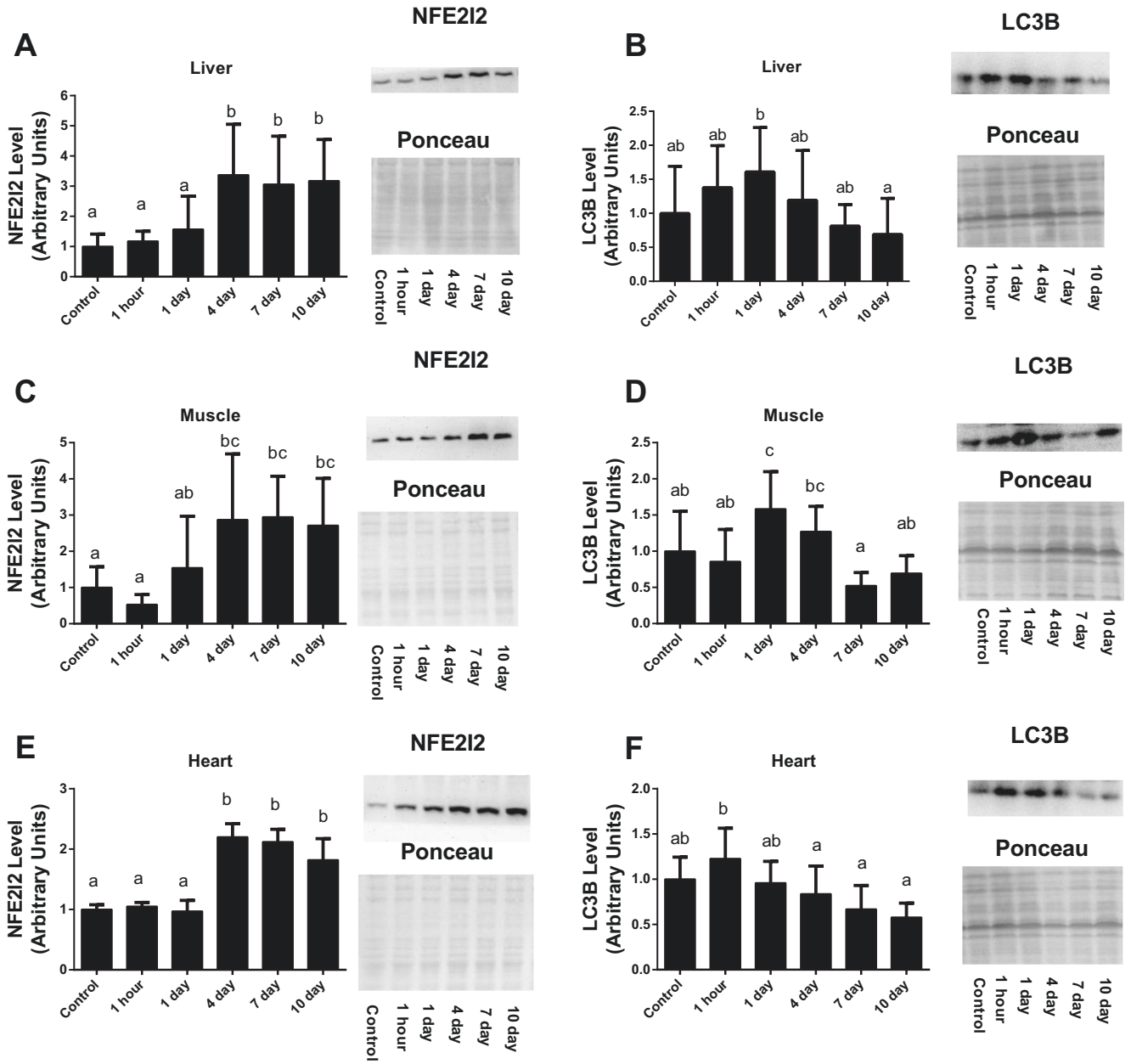

Fig. 5. Relative nuclear factor E2-related factor 2 (NFE2l2) and microtubule-associated proteins 1A/1B light chain 3B (LC3B) expression in liver (*A* and *B*, respectively), muscle (*C* and *D*, respectively), and heart (*E* and *F*, respectively) of house mice. Tissues were collected from nonirradiated control mice and from mice, 1 h and 1, 4, 7, and 10 days postirradiation. SD bars are given (n = 8/group). Bars with different superscripts are significantly different. Representative Western blot images are shown to the right of the graphs.

No significant differences were found for CuZnSOD and MnSOD (Fig. 8).

DISCUSSION

Overview of findings. AfterX-irradiation was completed, we observed an acute increase in liver and muscle mitochondrial ROS emission, but it dropped below control levels at *day 10* postirradiation. Importantly, markers of lipid and protein oxidation increased following X-ray exposure but then returned to control levels at *day 10* postirradiation. In addition, the expression of NFE2l2 increased after radiation exposure, suggesting that an upregulation of this protein may have played a regulatory role that prevented further damage. The consistency of these patterns across tissues suggests that an acute and brief oxidative event has the potential to improve cellular oxidative status.

ROS emission and oxidative damage. Ionizing radiation causes the immediate ionization of water, leading to the formation of H_2O_2 (44), but it can also cause organelle and cell damage that can lead to subsequent mitochondrial ROS emission, mainly due to superoxide production that can readily be converted to H_2O_2 (60). For example, Yamaguchi and Kashiwakura (59) found a sevenfold increase in ROS that was sustained for 3 days following 4 Gy X-irradiation but dropped back to control level at *day 7*. More interestingly, our data suggest that mitochondrial H_2O_2 production dropped below

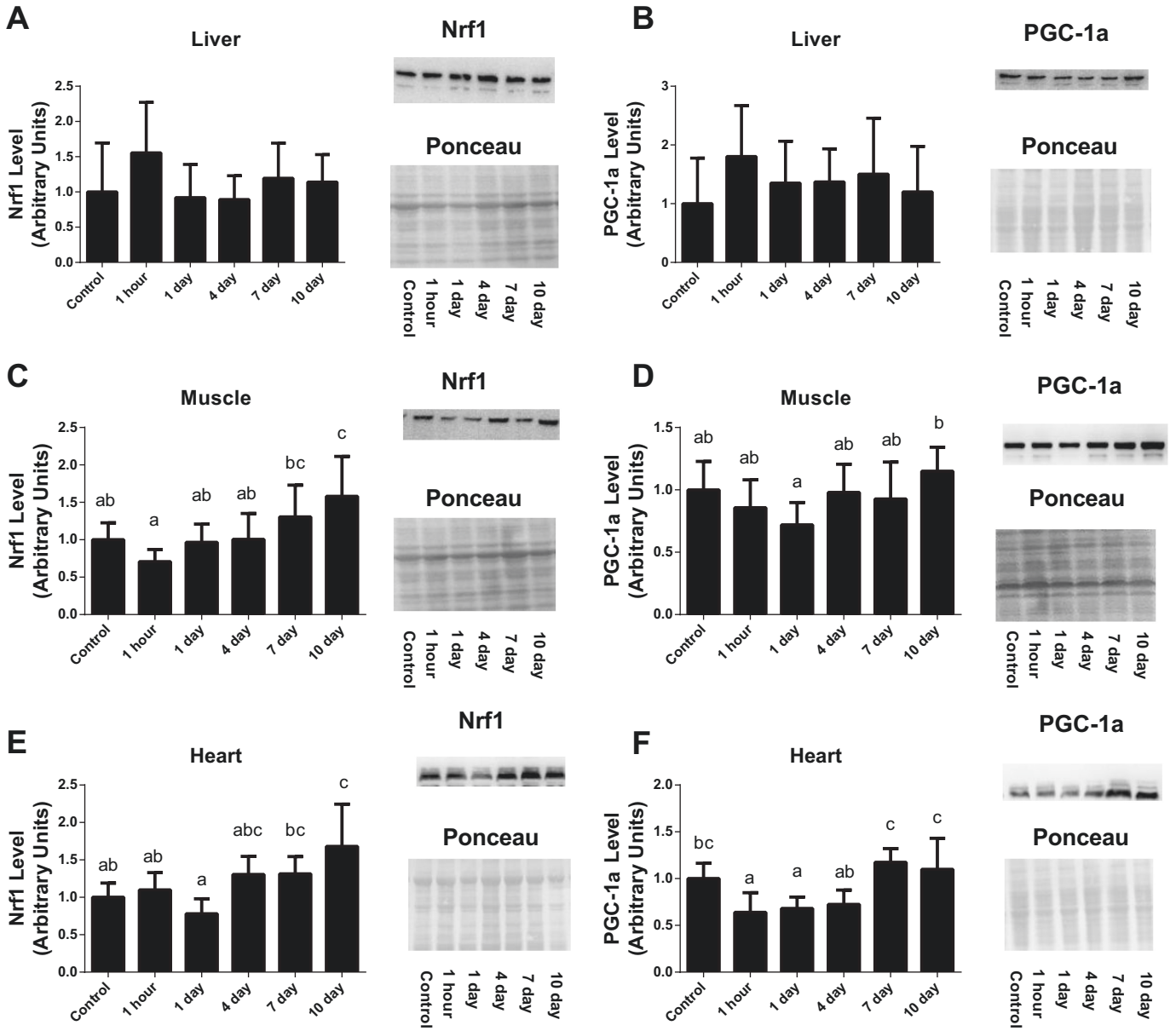

Fig. 6. Relative nuclear respiratory factor (Nrf1) and peroxisome proliferator-activated receptor gamma coactivator 1-α (PGC-1α) expression in liver (*A* and *B*, respectively), muscle (*C* and *D*, respectively), and heart (*E* and *F*, respectively) of mice. Tissues were collected from nonirradiated control mice and from mice, 1 h and 1, 4, 7, and 10 days postirradiation. SD bars are given (n = 8/group). Bars with different superscripts are significantly different. Representative Western blot images are shown to the right of the graphs.

control levels by 7 and 10 days postexposure in the muscle and liver, respectively. When production of ROS exceeds the capacity of an antioxidant defense system, then oxidative damage is inevitable. Oxidative damage can be divided into oxidative DNA damage, lipid peroxidation, and protein carbonylation (9). For this study, we focused on the latter two variables. Lipid peroxidation and protein carbonylation, in all four tissues, followed a concave pattern, with damage increasing and then dropping to or below control levels. Long-term studies have shown sustained damage following high dosages of irradiation and the return to pre-exposure levels following low-level X-ray exposure (20, 43). In contrast to this study, Datta et al. (8) observed an increase of lipid peroxidation in the intestinal epithelial cells, 1 yr following mild irradiation (2 Gy) in mice. The reason for the long-lasting effects was not clear, but it is possible that the cell of older mice does not respond in the same manner as younger individuals (9).

We can only speculate why protein carbonylation in the liver and muscle was lower than that of the unexposed controls on 10 days postexposure, which is consistent with other studies (30, 31). Possible explanations for this finding include the following: *1*) accelerated protein turnover (33) and *2*) degradation of oxidized protein by lysosomes/vacuole (autophagy) (56). In this study, the protein levels of an autophagy marker, LC3B, was higher after radiation and then dropped back to the control level at *day 10*. This observation may suggest that autophagy plays a role in radiation-induced mitohormesis, but future experiments must be performed to confirm this response.

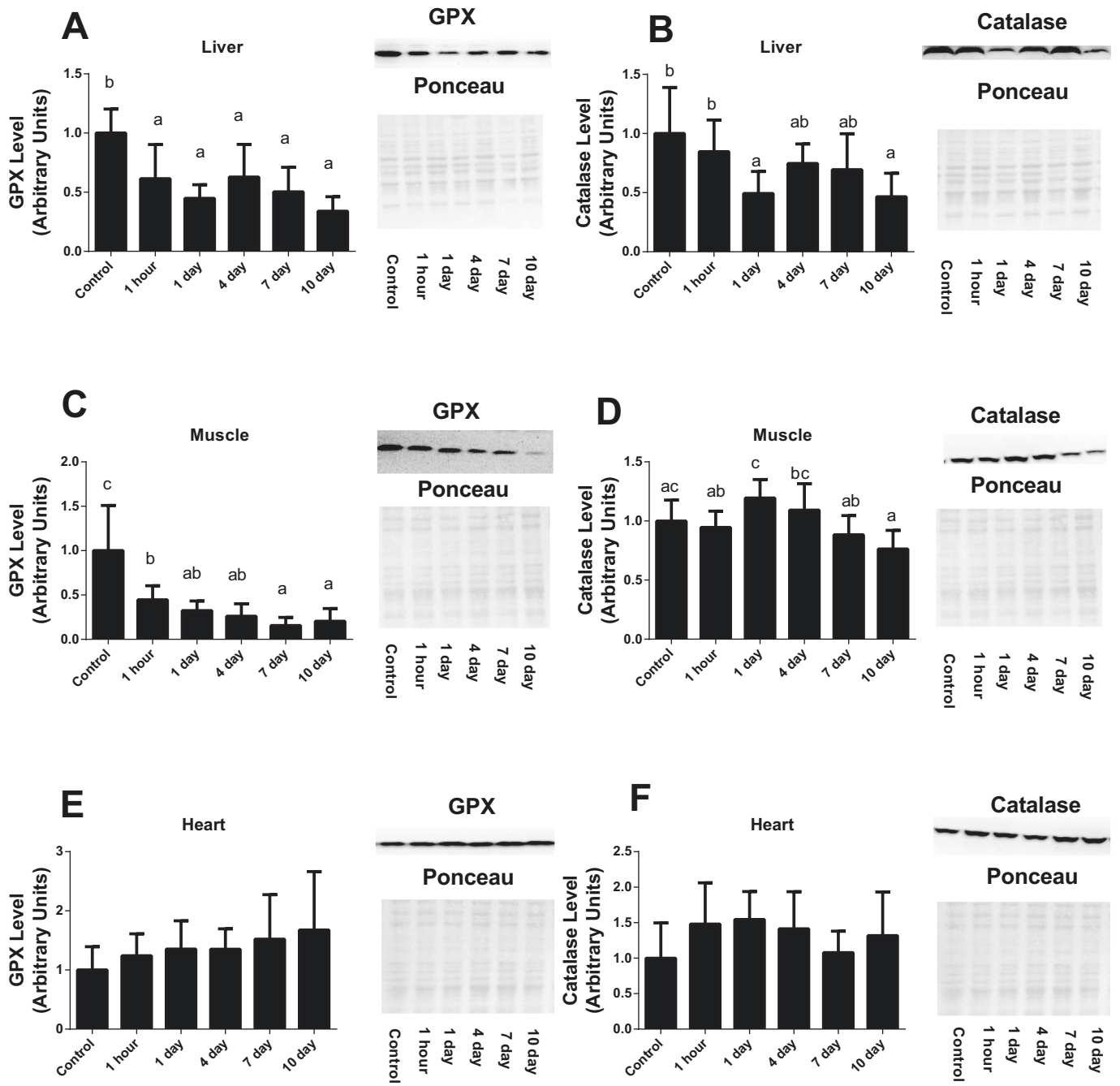

Fig. 7. Relative glutathione peroxidase 1 (GPX-1) and catalase expression in the liver (*A* and *B*, respectively), muscle (*C* and *D*, respectively), and heart (*E* and *F*, respectively) of mice. Tissues were collected from nonirradiated control mice and from mice, 1 h and 1, 4, 7, and 10 days postirradiation. SD bars are given (n = 8/group). Bars with different superscripts are significantly different. Representative Western blot images are shown to the right of the graphs.

Mitochondrial function and complex activities. Liver mitochondria function (i.e., RCR using complex I substrates) displayed a convex pattern that was the inverse of oxidative damage. Similar trends, albeit not significant, were observed in liver mitochondria with the complex II substrate and in muscle mitochondria with complex I substrates. It appears that the liver is more responsive and susceptible to damage than skeletal muscles under many conditions (23, 41). Furthermore, as a postmitotic tissue, skeletal muscles are terminally differentiated and have a relatively slow turnover rate (6, 37). These patterns imply that the increase in lipid and protein damage can have a direct effect on mitochondrial respiratory capacity. To our best knowledge, this study is the first to quantify the temporal change in RCR following oxidant exposure in mammals. Mitochondrial complex activities have been proposed to be one of the important indicators for mitochondrial function (54), and our findings support this notion for liver. The activities of complexes I, III, and IV in the liver were upregulated, 7 and 10 days post-X-irradiation, and similar findings have been documented by previous investigators (60). It is not clear why the function of liver mitochondria with the complex II substrate was not affected by radiation as much as with the

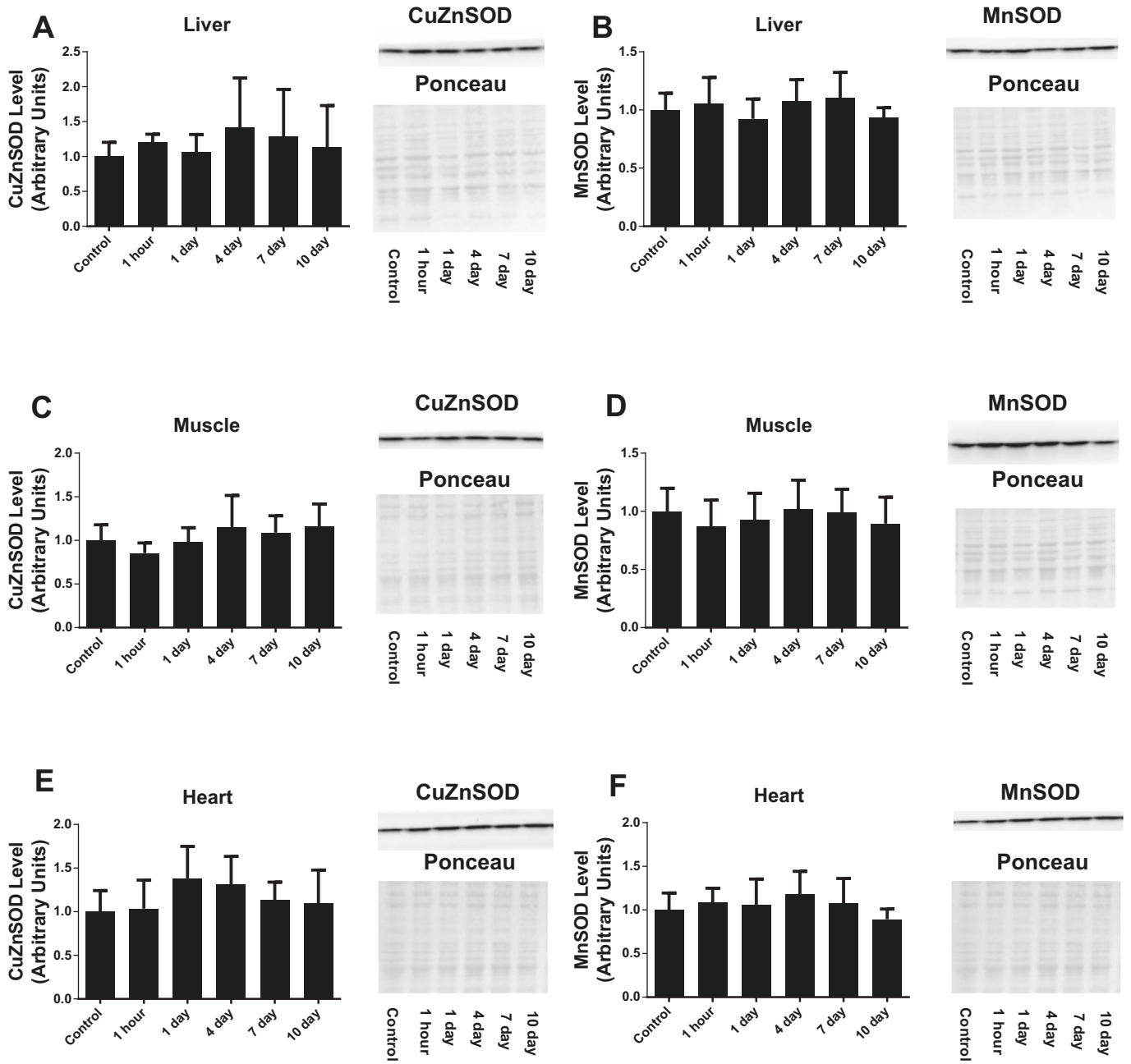

Fig. 8. Relative copper-zinc SOD (CuZnSOD) and manganese SOD (MnSOD) expression in the liver (*A* and *B*, respectively), muscle (*C* and *D*, respectively), heart (*E* and *F*, respectively) of mice. Tissues were collected from nonirradiated control mice and from mice, 1 h and 1, 4, 7, and 10 days postirradiation. SD bars are given (n = 8/group). Representative Western blot images are shown to the right of the graphs.

complex I substrate. Each substrate uses a different transporter to cross the mitochondrial membrane, and this may have contributed to the difference in performance. It is also important to note that mitochondrial content, as estimated by CS activities in liver, muscle, and heart, did not differ at any time points in the study.

NFE2l2 is a mediator of the response to irradiation. NFE2l2 is a transcriptional factor that upregulates genes involved in mitochondrial integrity, OXPHOS efficiency, mitochondrial biogenesis, and DNA repair (10, 24, 26). Radiation has been shown to activate NFE2l2 previously (35, 49). In this study, the upregulation of the active form of NFE2l2 was observed in liver, muscle, and heart, 4 days following irradiation, and upregulation was maintained at least 10 days postexposure in all tissue. An increase of NFE2l2 indicated that the antioxidant system was upregulated after irradiation to protect cells and organelles from oxidative stress. 4-HNE is a possible activator of NFE2l2 (32). In this study, increased levels of 4-HNE protein product at *day 1* were likely responsible for the observed upregulation of NFE2l2, and subsequently, the drop in lipid and protein oxidative damage could have been a response to NFE2l2-level upregulation. Given the consistency and strength of the NFE2l2 response, it is probable that this regulatory factor plays a important role in the recovery and

improved performance of mitochondria following radiation. Moreover, markers for mitochondrial biogenesis were also upregulated at *day 10* compared with 1 h or 1 day postirradiation in muscle and heart but not in liver. However, mitochondrial content, indicated by CS activities, did not vary among groups.

Application and future directions. Oxidative stress has been proposed to underlie a diverse range of biological phenomena, including aging, cancer, muscle performance, ornament production, and life history evolution (11, 18, 38, 42, 53). Even as biologists acknowledge the central role of mitochondria as centers of release and regulation of free radicals, all too often, mitochondrial processes are characterized as one-dimensional parameters that can be characterized with measurements taken at one time point. Here, we show that mitochondrial responses to ROS production are anything but simple. We show that soon after X-ray exposure, there is an initial spike in the relative mitochondrial ROS emission and oxidative damage, but these values fall at or below pre-exposure levels within 0.5–1.5 wk after irradiation. These observations provide strong support for the idea that ROS do not merely cause harm but also signal changes within the cell that help the system to adapt to a change in redox conditions.

Many explanations for the role of ROS and oxidative stress in biological processes lack rigorous testing. This study provides a framework for understanding how cells respond to an oxidative event in natural systems. We found that acute ROS exposure can alter core respiratory processes in a manner that reduces damage and that should allow an organism to respond appropriately to future internal and external stressors. In the field of evolutionary and ecological physiology, many researchers quantify oxidative stress in a single tissue—most often blood—at a single time point and assume that an increase in oxidative stress is associated with persistent negative impacts on an individual's performance (62). This study clearly shows that assumption can be false. This study also suggests that mitochondrial respiratory function, ROS production, and oxidative damage are relatively similar across organs following acute pro-oxidant exposure. It is also important to note here that oxidative challenge in this study was brief, and possibly long-term oxidative challenge might lead to different results. Whereas this shows that organs throughout the body may respond in a relatively similar manner when exposed to an acute oxidant, other studies suggest that different organs may respond differently to chronic changes in ROS production (5, 52, 53). Thus we urge our readers not to assume that the changes that occur in one organ are indicative of how other organs will respond to the same oxidative event.

Perspectives and Significance.

Whereas our study reveals the need for broader characterization of responses to pro-oxidant exposure, more studies are needed to characterize the processes that are involved in the cellular and organism response to oxidative stress and the processes that are involved in mitohormesis. Future studies should consider mitochondrial turnover, mitochondrial DNA damage and repair, mitophagy, apoptosis, and mitochondrial biogenesis. Moreover, prolonged oxidative challenges should be performed to study any potential hormetic effects on mitochondrial function, aging, and mortality. In short, the results of this study have important implications for many aspects of mitochondrial and oxidative stress research.

ACKNOWLEDGMENTS

The authors thank Adam Brasher, Christine Kallenberg, Emily Welling, Halie Taylor, Hayden Hyatt, and Michael Roberts for technical support in the laboratory. The authors also thank members of the W. R. Hood and Geoffrey Hill laboratory (Auburn University) groups for giving feedback on an early version of this paper.

GRANTS

Funding for this research was provided by the US National Science Foundation Grant 1453784 and the National Institutes of Health Grant R03 HD083654-01.

DISCLOSURES

No conflicts of interest, financial or otherwise, are declared by the authors.

AUTHOR CONTRIBUTIONS

Y.Z., A.N.K., and W.R.H. conceived and designed research; Y.Z., F.H., and G.A. performed experiments; Y.Z. analyzed data; Y.Z., A.N.K., and W.R.H. interpreted results of experiments; Y.Z. prepared figures; Y.Z. and W.R.H. drafted manuscript; Y.Z., A.N.K., and W.R.H. edited and revised manuscript; Y.Z., A.N.K., and W.R.H. approved final version of manuscript.

REFERENCES

1. **Beckman KB, Ames BN.** The free radical theory of aging matures. *Physiol Rev* 78: 547–581, 1998.
2. **Bratic I, Trifunovic A.** Mitochondrial energy metabolism and ageing. *Biochim Biophys Acta* 1797: 961–967, 2010. doi:10.1016/j.bbabio.2010.01.004.
3. **Calabrese EJ.** The maturing of hormesis as a credible dose-response model. *Nonlinearity Biol Toxicol Med* 1: 319–343, 2003. doi:10.1080/15401420390249907.
4. **Calabrese EJ, Baldwin LA.** Toxicology rethinks its central belief. *Nature* 421: 691–692, 2003. doi:10.1038/421691a.
5. **Cattan V, Mercier N, Gardner JP, Regnault V, Labat C, Mäki-Jouppila J, Nzietchueng R, Benetos A, Kimura M, Aviv A, Lacolley P.** Chronic oxidative stress induces a tissue-specific reduction in telomere length in CAST/Ei mice. *Free Radic Biol Med* 44: 1592–1598, 2008. doi:10.1016/j.freeradbiomed.2008.01.007.
6. **Crane JD, Abadi A, Hettinga BP, Ogborn DI, MacNeil LG, Steinberg GR, Tarnopolsky MA.** Elevated mitochondrial oxidative stress impairs metabolic adaptations to exercise in skeletal muscle. *PLoS One* 8: e81879, 2013. doi:10.1371/journal.pone.0081879.
7. **Croteau DL, Bohr VA.** Repair of oxidative damage to nuclear and mitochondrial DNA in mammalian cells. *J Biol Chem* 272: 25409–25412, 1997. doi:10.1074/jbc.272.41.25409.
8. **Datta K, Suman S, Kallakury BV, Fornace AJ Jr.** Exposure to heavy ion radiation induces persistent oxidative stress in mouse intestine. *PLoS One* 7: e42224, 2012. doi:10.1371/journal.pone.0042224.
9. **Davies KJ.** Oxidative stress, antioxidant defenses, and damage removal, repair, and replacement systems. *IUBMB Life* 50: 279–289, 2000. doi:10.1080/15216540051081010.
10. **Dinkova-Kostova AT, Abramov AY.** The emerging role of Nrf2 in mitochondrial function. *Free Radic Biol Med* 88: 179–188, 2015. doi:10.1016/j.freeradbiomed.2015.04.036.
11. **Finkel T, Holbrook NJ.** Oxidants, oxidative stress and the biology of ageing. *Nature* 408: 239–247, 2000. doi:10.1038/35041687.
12. **Friguet B.** Oxidized protein degradation and repair in ageing and oxidative stress. *FEBS Lett* 580: 2910–2916, 2006. doi:10.1016/j.febslet.2006.03.028.
13. **Galván I, Bonisoli-Alquati A, Jenkinson S, Ghanem G, Wakamatsu K, Mousseau TA, Møller AP.** Chronic exposure to low-dose radiation at Chernobyl favours adaptation to oxidative stress in birds. *Funct Ecol* 28: 1387–1403, 2014. doi:10.1111/1365-2435.12283.
14. **Garratt M, Vasilaki A, Stockley P, McArdle F, Jackson M, Hurst JL.** Is oxidative stress a physiological cost of reproduction? An experimental test in house mice. *Proc Biol Sci* 11: 1098–1106, 2011.
15. **Handy DE, Loscalzo J.** Redox regulation of mitochondrial function. *Antioxid Redox Signal* 16: 1323–1367, 2012. doi:10.1089/ars.2011.4123.

16. **Harman D.** Free radical theory of aging: an update: increasing the functional life span. *Ann NY Acad Sci* 1067: 10–21, 2006. doi:10.1196/annals.1354.003.
17. **Harper JM.** Wild-derived mouse stocks: an underappreciated tool for aging research. *Age (Dordr)* 30: 135–145, 2008. doi:10.1007/s11357-008-9057-0.
18. **Hill GE.** Cellular respiration: the nexus of stress, condition, and ornamentation. *Integr Comp Biol* 54: 645–657, 2014. doi:10.1093/icb/icu029.
19. **Hyatt HW, Kephart WC, Holland AM, Mumford P, Mobley CB, Lowery RP, Roberts MD, Wilson JM, Kavazis AN.** A ketogenic diet in rodents elicits improved mitochondrial adaptations in response to resistance exercise training compared to an isocaloric Western diet. *Front Physiol* 7: 533, 2016. doi:10.3389/fphys.2016.00533.
20. **Jagetia GC, Baliga MS, Venkatesh P, Ulloor JN.** Influence of ginger rhizome (Zingiber officinale Rosc) on survival, glutathione and lipid peroxidation in mice after whole-body exposure to gamma radiation. *Radiat Res* 160: 584–592, 2003. doi:10.1667/RR3057.
21. **Kavazis AN, Talbert EE, Smuder AJ, Hudson MB, Nelson WB, Powers SK.** Mechanical ventilation induces diaphragmatic mitochondrial dysfunction and increased oxidant production. *Free Radic Biol Med* 46: 842–850, 2009. doi:10.1016/j.freeradbiomed.2009.01.002.
23. **Kayatekin BM, Gönenç S, Açikgöz O, Uysal N, Dayi A.** Effects of sprint exercise on oxidative stress in skeletal muscle and liver. *Eur J Appl Physiol* 87: 141–144, 2002. doi:10.1007/s00421-002-0607-3.
24. **Kim SB, Pandita RK, Eskiocak U, Ly P, Kaisani A, Kumar R, Cornelius C, Wright WE, Pandita TK, Shay JW.** Targeting of Nrf2 induces DNA damage signaling and protects colonic epithelial cells from ionizing radiation. *Proc Natl Acad Sci USA* 109: E2949–E2955, 2012. doi:10.1073/pnas.1207718109.
25. **Koch RE, Hill GE.** An assessment of techniques to manipulate oxidative stress in animals. *Funct Ecol* 31: 9–21, 2017. doi:10.1111/1365-2435.12664.
26. **Kwak M-K, Wakabayashi N, Itoh K, Motohashi H, Yamamoto M, Kensler TW.** Modulation of gene expression by cancer chemopreventive dithiolethiones through the Keap1-Nrf2 pathway. Identification of novel gene clusters for cell survival. *J Biol Chem* 278: 8135–8145, 2003. doi:10.1074/jbc.M211898200.
27. **Lane N.** *Oxygen: The Molecule That Made the World*. Oxford, UK: Oxford University Press, 2002.
28. **Leach JK, Van Tuyle G, Lin PS, Schmidt-Ullrich R, Mikkelsen RB.** Ionizing radiation-induced, mitochondria-dependent generation of reactive oxygen/nitrogen. *Cancer Res* 61: 3894–3901, 2001.
29. **Lee Y, Min K, Talbert EE, Kavazis AN, Smuder AJ, Willis WT, Powers SK.** Exercise protects cardiac mitochondria against ischemia-reperfusion injury. *Med Sci Sports Exerc* 44: 397–405, 2012. doi:10.1249/MSS.0b013e318231c037.
30. **López-Martínez G, Hahn DA.** Early life hormetic treatments decrease irradiation-induced oxidative damage, increase longevity, and enhance sexual performance during old age in the Caribbean fruit fly. *PLoS One* 9: e88128, 2014. doi:10.1371/journal.pone.0088128.
31. **López-Martínez G, Hahn DA.** Short-term anoxic conditioning hormesis boosts antioxidant defenses, lowers oxidative damage following irradiation and enhances male sexual performance in the Caribbean fruit fly, Anastrepha suspensa. *J Exp Biol* 215: 2150–2161, 2012. doi:10.1242/jeb.065631.
32. **Ma Q.** Role of nrf2 in oxidative stress and toxicity. *Annu Rev Pharmacol Toxicol* 53: 401–426, 2013. doi:10.1146/annurev-pharmtox-011112-140320.
33. **Marques M, Mojzita D, Amorim MA, Almeida T, Hohmann S, Moradas-Ferreira P, Costa V.** The Pep4p vacuolar proteinase contributes to the turnover of oxidized proteins but PEP4 overexpression is not sufficient to increase chronological lifespan in *Saccharomyces cerevisiae*. *Microbiology* 152: 3595–3605, 2006. doi:10.1099/mic.0.29040-0.
34. **Mattson MP.** Hormesis defined. *Ageing Res Rev* 7: 1–7, 2008. doi:10.1016/j.arr.2007.08.007.
35. **McDonald JT, Kim K, Norris AJ, Vlashi E, Phillips TM, Lagadec C, Della Donna L, Ratikan J, Szelag H, Hlatky L, McBride WH.** Ionizing radiation activates the Nrf2 antioxidant response. *Cancer Res* 70: 8886–8895, 2010. doi:10.1158/0008-5472.CAN-10-0171.
36. **Metcalfe NB, Alonso-Alvarez C.** Oxidative stress as a life-history constraint: the role of reactive oxygen species in shaping phenotypes from conception to death. *Funct Ecol* 24: 984–996, 2010. doi:10.1111/j.1365-2435.2010.01750.x.
37. **Miwa S, Lawless C, von Zglinicki T.** Mitochondrial turnover in liver is fast in vivo and is accelerated by dietary restriction: application of a simple dynamic model. *Aging Cell* 7: 920–923, 2008. doi:10.1111/j.1474-9726.2008.00426.x.
38. **Monaghan P, Metcalfe NB, Torres R.** Oxidative stress as a mediator of life history trade-offs: mechanisms, measurements and interpretation. *Ecol Lett* 12: 75–92, 2009. doi:10.1111/j.1461-0248.2008.01258.x.
39. **Mowry AV, Kavazis AN, Sirman AE, Potts WK, Hood WR.** Reproduction does not adversely affect liver mitochondrial respiratory function but results in lipid peroxidation and increased antioxidants in house mice. *PLoS One* 11: e0160883, 2016. doi:10.1371/journal.pone.0160883.
40. **Nguyen T, Nioi P, Pickett CB.** The Nrf2-antioxidant response element signaling pathway and its activation by oxidative stress. *J Biol Chem* 284: 13291–13295, 2009. doi:10.1074/jbc.R900010200.
41. **Porta F, Takala J, Weikert C, Bracht H, Kolarova A, Lauterburg BH, Borotto E, Jakob SM.** Effects of prolonged endotoxemia on liver, skeletal muscle and kidney mitochondrial function. *Crit Care* 10: R118, 2006. doi:10.1186/cc5013.
42. **Powers SK, Jackson MJ.** Exercise-induced oxidative stress: cellular mechanisms and impact on muscle force production. *Physiol Rev* 88: 1243–1276, 2008. doi:10.1152/physrev.00031.2007.
43. **Rejholcová M, Wilhelm J, Rejholcova M.** Time course of lipolytic activity and lipid peroxidation after whole-body gamma irradiation of rats. *Radiat Res* 117: 21–25, 1989. doi:10.2307/3577273.
44. **Riley PA.** Free radicals in biology: oxidative stress and the effects of ionizing radiation. *Int J Radiat Biol* 65: 27–33, 1994. doi:10.1080/09553009414550041.
45. **Risom L, Møller P, Vogel U, Kristjansen PE, Loft S.** X-Ray-induced oxidative stress: DNA damage and gene expression of HO-1, ERCC1 and OGG1 in mouse lung. *Free Radic Res* 37: 957–966, 2003. doi:10.1080/1071576031000150788.
46. **Ristow M.** Unraveling the truth about antioxidants: mitohormesis explains ROS-induced health benefits. *Nat Med* 20: 709–711, 2014. doi:10.1038/nm.3624.
47. **Ristow M, Schmeisser K.** Mitohormesis: promoting health and lifespan by increased levels of reactive oxygen species (ROS). *Dose Response* 12: 288–341, 2014. doi:10.2203/dose-response.13-035.Ristow.
48. **Rugo RE, Schiestl RH.** Increases in oxidative stress in the progeny of X-irradiated cells. *Radiat Res* 162: 416–425, 2004. doi:10.1667/RR3238.
49. **Sekhar KR, Freeman ML.** Nrf2 promotes survival following exposure to ionizing radiation. *Free Radic Biol Med* 88: 268–274, 2015. doi:10.1016/j.freeradbiomed.2015.04.035.
50. **Sena LA, Chandel NS.** Physiological roles of mitochondrial reactive oxygen species. *Mol Cell* 48: 158–167, 2012. doi:10.1016/j.molcel.2012.09.025.
51. **Sies H.** Oxidative stress: introductory remarks. In: *Oxidative Stress*, edited by Sies H. London: Academic, 1985, p. 1–8.
52. **Speakman JR, Blount JD, Bronikowski AM, Buffenstein R, Isaksson C, Kirkwood TBL, Monaghan P, Ozanne SE, Beaulieu M, Briga M, Carr SK, Christensen LL, Cochemé HM, Cram DL, Dantzer B, Harper JM, Jurk D, King A, Noguera JC, Salin K, Sild E, Simons MJP, Smith S, Stier A, Tobler M, Vitikainen E, Peaker M, Selman C.** Oxidative stress and life histories: unresolved issues and current needs. *Ecol Evol* 5: 5745–5757, 2015. doi:10.1002/ece3.1790.
53. **Speakman JR, Garratt M.** Oxidative stress as a cost of reproduction: beyond the simplistic trade-off model. *BioEssays* 36: 93–106, 2014. doi:10.1002/bies.201300108.
54. **Spinazzi M, Casarin A, Pertegato V, Salviati L, Angelini C.** Assessment of mitochondrial respiratory chain enzymatic activities on tissues and cultured cells. *Nat Protoc* 7: 1235–1246, 2012. doi:10.1038/nprot.2012.058.
55. **Szumiel I.** Radiation hormesis: autophagy and other cellular mechanisms. *Int J Radiat Biol* 88: 619–628, 2012. doi:10.3109/09553002.2012.699698.
56. **Thorpe GW, Fong CS, Alic N, Higgins VJ, Dawes IW.** Cells have distinct mechanisms to maintain protection against different reactive oxygen species: oxidative-stress-response genes. *Proc Natl Acad Sci USA* 101: 6564–6569, 2004. doi:10.1073/pnas.0305888101.
57. **Tothova Z, Kollipara R, Huntly BJ, Lee BH, Castrillon DH, Cullen DE, McDowell EP, Lazo-Kallanian S, Williams IR, Sears C, Armstrong SA, Passegué E, DePinho RA, Gilliland DG.** FoxOs are critical mediators of hematopoietic stem cell resistance to physiologic oxidative stress. *Cell* 128: 325–339, 2007. doi:10.1016/j.cell.2007.01.003.
58. **Williams JP, Brown SL, Georges GE, Hauer-Jensen M, Hill RP, Huser AK, Kirsch DG, Macvittie TJ, Mason KA, Medhora MM, Moulder JE, Okunieff P, Otterson MF, Robbins ME, Smathers JB,**

McBride WH. Animal models for medical countermeasures to radiation exposure. *Radiat Res* 173: 557–578, 2010. doi:10.1667/RR1880.1.

59. **Yamaguchi M, Kashiwakura I.** Role of reactive oxygen species in the radiation response of human hematopoietic stem/progenitor cells. *PLoS One* 8: e70503, 2013. doi:10.1371/journal.pone.0070503.
60. **Yamamori T, Yasui H, Yamazumi M, Wada Y, Nakamura Y, Nakamura H, Inanami O.** Ionizing radiation induces mitochondrial reactive oxygen species production accompanied by upregulation of mitochondrial electron transport chain function and mitochondrial content under control of the cell cycle checkpoint. *Free Radic Biol Med* 53: 260–270, 2012. doi:10.1016/j.freeradbiomed.2012.04.033.
61. **Yun J, Finkel T.** Mitohormesis. *Cell Metab* 19: 757–766, 2014. doi:10.1016/j.cmet.2014.01.011.
62. **Zhang Y, Hood WR.** Current versus future reproduction and longevity: a re-evaluation of predictions and mechanisms. *J Exp Biol* 219: 3177–3189, 2016. doi:10.1242/jeb.132183.